doi.org/10.36721/PJPS.2023.36.1.REG.111-119.1

Prediction of Covid-19 symptoms with chest x-ray to optimize the solution through the MCOA Algorithm for feature extraction and measurement

Prabhakaran Natrajan[1], Anandha Prasad Sekar[2], Kamali Murugan[2], Chandrasekar Sabarinathan[3], Inbaraj Chandra[4] and Venkatesan Prabhu[5]

[1]Department of Biomedical Engineering, Agni College of Technology, Chennai, India
[2]Department of ECE, Vel Tech High Tech Dr. Rangarajan Dr. Sakunthala Engineering College, Chennai, India
[3]Department of CSE, SRM University, Vadapalani Campus, India
[4]Department of ECE, Rajalakshmi Institute of Technology, Thandalam, Chennai, India
[5]Department of ECE, Vel Tech Multi Tech Dr. Rangarajan Dr. Sakunthala Engineering College, Chennai, India

Abstract: Due to poor understanding and inconsistent knowledge about covid-19 symptoms, the survival rate will decrease anywhere in the world. Every person who lives in the world should aware of COVID-19 symptoms to protect their life and hence increase the mortality rate of humans. The Indian government took precautions to lower the fatality rate, which includes hand sanitizer, wearing NS2 masks and keeping social distance to live a long life. The proposed method uses the MCOA-modified cat optimization algorithm to extract the image features and predict them in earlier stages and diagnosis. Furthermore, the proposed method clusters the chest image concerning size, shape and intensity concerning the irregular edges present in the chest imaging. The proposed MCAO algorithm cluster the chest image with an accuracy of about 95% and fit into the solution space with the state of art. The problem of the concave region present in the image is clustered in the solution space to delineate the parameters of pneumonia, fever, mucus fluid and respiration rate. The method gives the solution to the radiologist to detect earlier covid 19 symptoms for feature extraction and measurement

Keywords: Survival rate, covid-19, MCOA, and chest X-ray imaging.

INTRODUCTION

The COVID-19 pandemic spreads through the air and infects many people who live around the world. The issue of COVID-19 symptoms is being investigated by radiologists, scientists, and researchers, with the aid of reducing virus spread and mortality rate. The parameter analyzed for the symptoms of covid includes fever, cough, headache, pneumonia and respiratory rate, which affects the entire lung system. The 3 tests used to detect COVID-19 symptoms are computed tomography, RT-PCR, and ultrasound imaging. Furthermore, all these 3 test analyses only after the symptoms of covid, but the proposed method includes earlier detection of COVID-19 symptoms. The 3-D radiographic image is analyzed by computed tomography which forecasts each pixel by false positives, false negatives, true positives and true negatives. Similar to RT-PCR, which is prone to human error and identifies the symptoms of covid in reverse transcription and plasma treatment is also important to detect COVID-19 analysis. X-ray imaging takes less computational time to anticipate COVID-19 symptoms as early as feasible when compared to lung ultrasound. COVID-19 symptoms are more expensive than the then-current approach of testing. Nowadays, the medical industry suggested many solutions to the government of India, but all the steps are related to social distancing to safeguard their life. The clustering of chest X-ray images proves the early COVID-19 symptoms and accurate analysis with suggested parameters to fit into the solution space. The radiologist approach discovers and detects earlier analysis of covid with chest images based on citation scores. The significant characteristics will anticipate a clustering algorithm to enhance COVID-19 parameters of pneumonia, fever, mucus fluid and respiration rate. The DL algorithm enhances image features with high contrast image the high contrast image visualized by the radiologist as pixel strength represented as True Negative. X-Ray image does not diagnose the image as precisely. The COVID-19 patient's chest X-ray image is clustered using MCOA which predicts an accuracy of about 95% using. The radiography technology initially improves image characteristics and helps to emphasize the Medical Centre over specific uncertainty.

Related work

Kumar proposed covid-19 analysis about social distance and self-isolation of persons brought during the lockdown period. However, this technique cannot be assigned to achieve both indoor and outdoor ventilation systems (Djuric O *et al*., 2022). Erdem proposed 91 suitable adult patients categorized based on treatment in ICU, ward, or outpatient clinic. Second, based on computed tomography scores, the severity was classified (Erdem K *et al*., 2022) Freidman exhibited vaccines found to be immunogenic

*Corresponding author: e-mail: captainprabhakar1982@yahoo.co

and extremely effective in well-controlled clinical trials. The adult reporting seroconversion rates of an mRNA vaccine given to a cohort (Friedman-Klebanoff DAJ *et al*., 2022) The suggestion of the immune system with a high IL-6 response causes severe and systemic damage to the pathophysiological characteristics of COVID-19. Cytokines including interferon-gamma deemed good predictors of COVID-19 severity (Lo E *et al*., 2022). To launch the infectious outbreak and lower the fatality rate, Materassi proposed geometric motivation with apparent logistic specified equations (Materassi M *et al*., 2019). Maintaining social distancing and avoiding infection in frontline healthcare workers are two immediate steps that must be taken to halt the spread of the contagious disease covId-19 in daily life (McEniery CM *et al*., 2020) Mohammed's purpose of determining COVID-19 infection or vaccination status and the feasibility of blood sample collection methods for the presence of SARS-CoV-2 antibodies from the VA Military Veteran Program (MVP) was investigated (Mohammed T *et al*., 2022). Illustrated by sokas early-stage breast and prostate cancer patients' perspectives on surgical delays are discussed in cancer in the shadow of covid-19 (Sokas C *et al*., 2021). Suy proposed Coronavirus Disease illness has been affecting people worldwide since December 2019 and is a novel disease. There is conflicting evidence regarding SARS-impact CoV-2's on pregnant women (Suy A *et al*., 2021) Weller said that this was especially true in the field of neuro-oncology, where there is a generally low perception of the efficacy of therapeutic methods for treating brain tumors (Weller M *et al*., 2020). Wilke recommended analyzing the COVID-19 Pandemic's Effect on the Multidisciplinary Management of Breast Cancer: A Review from the Registries for COVID-19 and Mastery (Wilke LG *et al*., 2021). The issues in contour edge detection like pneumonia, temperature and suffocation, will detect Chest X-Ray imaging to define the features of an image. In contrast to other existing methods, the physician will make better decisions in contour edge detection to lower the mortality rate (Arias-Londono JD *et al*., 2020). Extraction through clustering algorithm will measure features in the pixel size and examine the CXR image based on concave region. X-Ray imaging predicts the signs despite the pleural alterations of concave region detection (Dong D *et al*., 2021). The kit analyses the mucus fluid associated with COVID-19 symptoms and predicts negative outcomes based on the test identified by the radiologist known as RT-PCR (Gharizadeh B *et al*., 2021). Understanding COVID-19 symptoms put the radiologist at high risk which differentiates normal and abnormal concave regions. The X-Ray imaging will cluster and classify the feature of the image (Jiang Y *et al*., 2021). Prior knowledge about segmentation and classification are labeled and unlabeled pixels will accurately identify the early symptoms (Joshi A *et al*., 2020). Inhomogeneity of pixels will remove noisy errors for contour in the region of interest (ROI) (Karadayi Y *et al*., 2020). However, the segmentation of a Computed Tomography (CT) picture using a matrix approach can also be used to assess the detection of COVID-19. The segmentation algorithm's virus detection accuracy is verified by the Computed Tomography image matrix approach (Lju Q *et al*., 2020). The modeling analysis stops viruses from spreading from one person to another and displays the remarkable structure of viruses in daily life, preserving human life from 45 to 80 years as identified by the researcher in the public database (Marmarelis VZ *et al*., 2020). he suggested segmentation technique can automatically extract the features of Chest X-Ray imaging analysis from a variety of datasets for public users (Peng Y *et al*., 2021). Pixel classification of supervised and unsupervised pictures is used to assess the performance of inhomogeneity and a non-contour edge detection technique significantly predicts image anomalies such as size, shape, and intensity (Rajaraman S *et al*., 2020). Inhomogeneity in the chest X-ray image, which is supported by false-negative pixels in the segmentation of the edge detection algorithm, predicts the future enhancement strategy (Sakib S *et al*., 2020). Despite the Edge detection method, the RT-PCR kit produces false negatives for clinical diagnoses, delaying the initiation of treatment. The supervised deep learning strategy initializes the diagnosis process and segments the pixel using contour edge detection to maximize the integrity of the solution space in the random variable of the low energy function (Shi J *et al*., 2020). The social distance is preserved by the Too Close Too Long (TCTL) Bluetooth low energy mode, which is also virus-free for longer life. According to the RSSI measurement and PACT measurement, Too Close for Too Long (TCTL) should be considered to maintain social distance even below 6 feet in solution space (Su Z *et al* 2021). COVER-1.0 increases the energy function by maintaining a distinct degree of hierarchical structure for the visual interpretation of Chest X-Ray imaging (Tabik S *et al*., 2020). Chest X-ray imaging improves the visual feature to gather a lot of changes in a short amount of time to show accuracy. The visual model for surveying and preventing the COVID-19 virus from propagating through the designated channels accurately matches the ACGAN model's accuracy forecasts for future imaging enhancement (Waheed A *et al*., 2020).

Methodology

The modified cat optimization algorithm clusters x-ray imaging to enhance the high features of the image in-order to delineate high-contrast images. Generally, the enhancement of features originates images based on pixel size, shape, intensity and probably pixel dimension. The clustered pixel is enhanced and optimized in the solution space. Furthermore, the cat optimization algorithm clusters the chest x-ray image for pixel dimension and the range of selected dimension from one pixel to another pixel. But the modified cat optimization algorithm cluster the pixel with the selected range and also it selects the pixel with irregular edge and boundary in the concave region and optimize the solution with high accuracy.

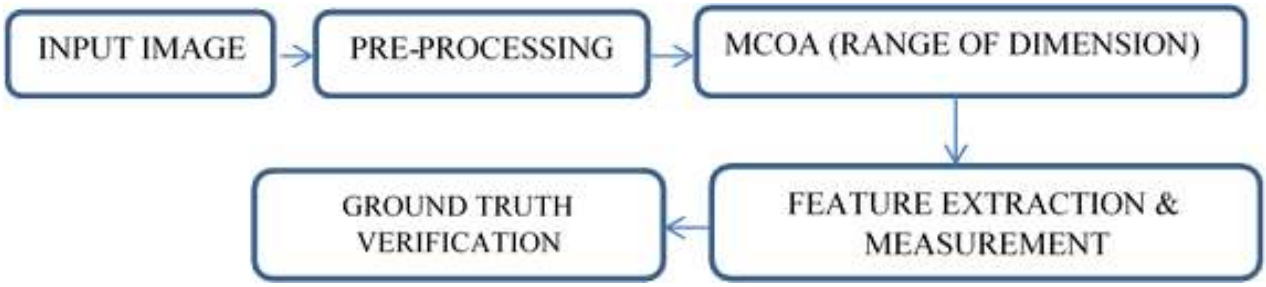

Fig. 1: Proposed block diagram of MCOA (modified cat optimization algorithm)

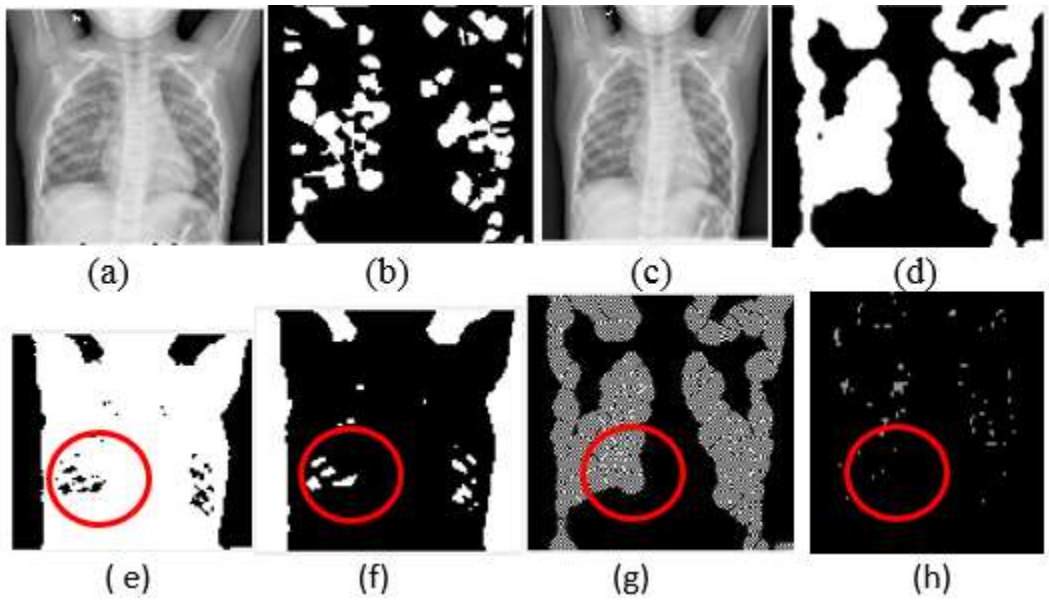

Fig. 2: (a) - (h) Infected person COVID-19 within 3 days- Chest X-Ray Imaging - image feature extracted through fever.

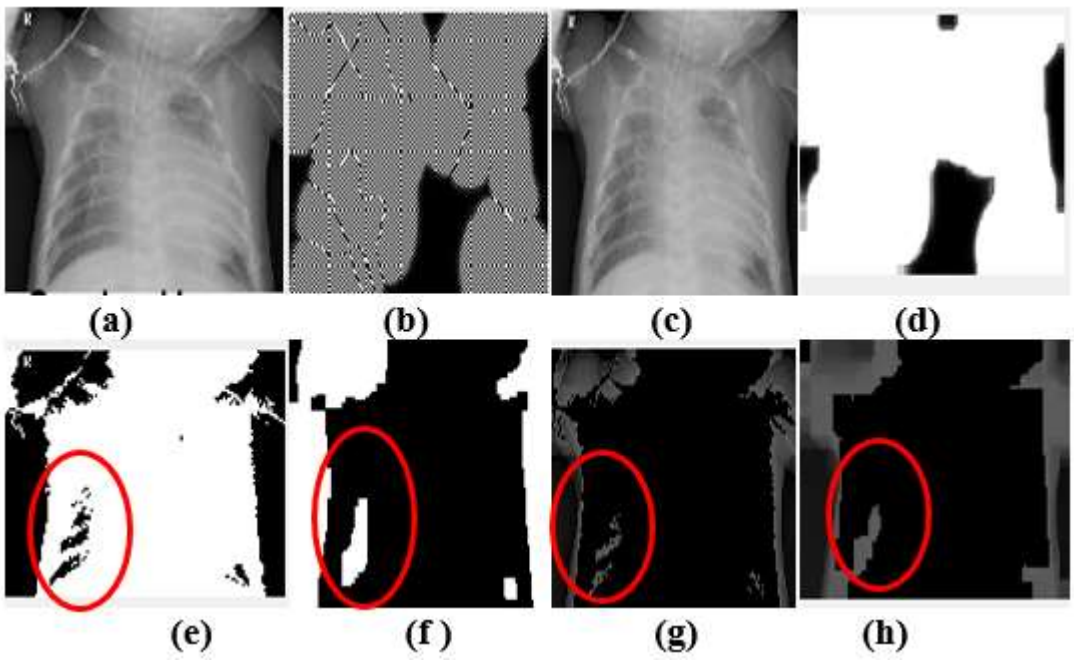

Fig. 3: (a) -(h) Spread occurs throughout the lungs within Six days -Chest X-ray, image parameter extracted through

Table 1: Statistical parameter of fever for the convex and concave region

.	Input		Contour boundary 1		Contour boundary 1		Contour boundary 1	
	Convex region	Non – Convex	Convex region	Non – Convex	Convex region	Non – Convex	Convex region	Non – Convex
Asymmetry	0.614	0.602	0.701	0.682	0.741	0.722	0.781	0.612
Compactness index	0.602	0.591	0.621	0.601	0.682	0.645	0.615	0.608
Dimension	0.599	0.543	0.636	0.598	0.676	0.634	0.648	0.591
Edge	0.532	0.506	0.589	0.545	0.624	0.604	0.518	0.502

Table 2: Parameter analysis for extraction of pneumonia.

	Image boundary		boundary 1		boundary 1		boundary 1	
	Convex region	Non – Convex	Convex region	Non – Convex	Convex region	Non – Convex	Convex region	Non – Convex
Asymmetry	0.618	0.594	0.648	0.645	0.658	0.649	0.648	0.684
Compactness	0.681	0.595	0.615	0.662	0.649	0.686	0.654	0.648
Dimension	0.691	0.535	0.672	0.618	0.654	0.618	0.617	0.615
Edge	0.657	0.618	0.648	0.648	0.648	0.656	0.605	0.604

Table 3: Parameter extraction - mucus fluid

	Input		Contour boundary 1		Contour boundary 1		Contour boundary 1	
	Convex region	Non - Convex	Convex region	Non - Convex	Convex region	Non - Convex	Convex region	Non - onvex
Asymmetry	0.618	0.622	0.641	0.675	0.647	0.674	0.698	0.678
Compactness	0.645	0.685	0.695	0.645	0.632	0.675	0.642	0.687
Dimension	0.648	0.635	0.674	0.699	0.641	0.632	0.645	0.685
Edge	0.628	0.647	0.696	0.644	0.674	0.610	0.646	0.695

Table 4: Parameter extraction respiration rate.

	Input		Contour boundary 1		Contour boundary 1		Contour boundary 1	
	Convex region	Non - Convex	Convex region	Non - Convex	Convex region	Non - Convex	Convex region	Non - onvex
Asymmetry	0.611	0.654	0.684	0.649	0.549	0.613	0.518	0.679
Compactness	0.615	0.625	0.585	0.532	0.548	0.546	0.618	0.619
Dimension	0.647	0.664	0.617	0.545	0.618	0.617	0.628	0.589
Edge	0.682	0.624	0.618	0.694	0.571	0.647	0.549	0.518

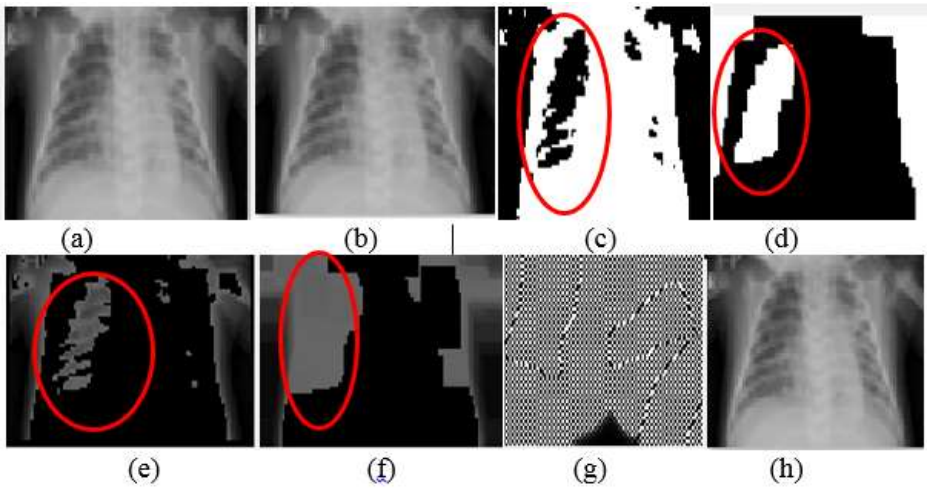

Fig. 4: (a) - (h) Spreadd infect the entire part of the lung before 9 days - Chest X-Ray, image parameter extracted through mucus fluid.

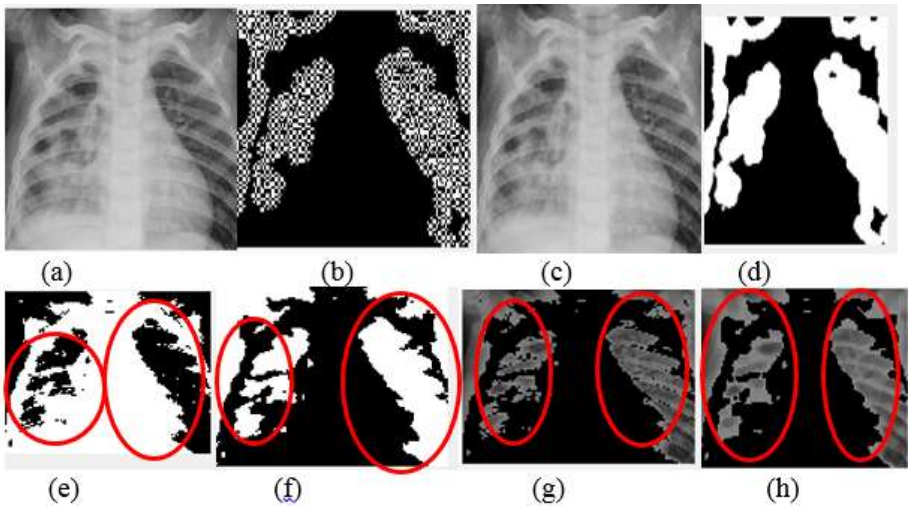

Fig. 5: (a) -(h) infection spread over all parts of the lungs -critical situation, image parameter extracted through respiration rate focus on final stages.

The modified cat optimization algorithm clusters the pixel in terms of two modes. The two modes are named seeking and tracing modes according to the initialization of the cat position with the neighborhood pixel in the selected dimension. Fig. 1 shows the proposed block diagram of the MCOA cluster and the chest x-ray image in the state of the art. Hence after the MCOA cluster, the process is extracted to cluster high image features as well to enhance the contrast and to reduce dimensional error are accurately predicted in this method. The problem of the proposed method clusters the concave region and finds the best optimal solution search space. After optimization of chest X-ray imaging, the obtained results are verified concerning the ground truth verification.

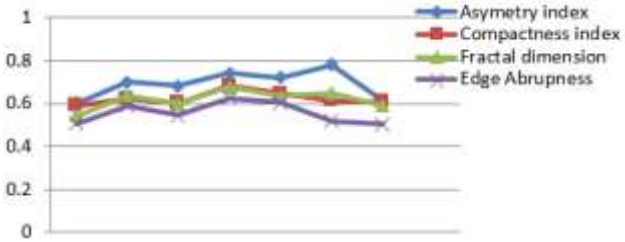

Fig. 6: Parameter extracted for fever in chest X-Ray

Fig. 2 shows the virus-affected person within 3 days from the extracted parameter of fever. The MCOA clusters the image concerning the image dimension and range of selection of pixels with inner and outer boundary prediction. The image is processed through certain types of filters where the noise is eliminated to enhance high-contrast clustered images. The clustered image is the noise-free image which reduces pepper and salt noise and improves the accuracy in the solution space. Thus by comparing the fig. from (a) to (h) we find changes in all the images. The changes are enhanced with high image features to obtain the best optimal solution in search space by local optima. When comparing fig. (a) to (e) the portion highlighted in red color indicates some parts of the lungs the infection rate is slightly increased which are highlighted and marked in red color. Furthermore, when comparing fig. (a) to (f) how far the virus affects the lung region and how it spreads randomly. Fig. (g) accurately represents the pixel with the right side of the lungs affected within the region of contrast. By analyzing the pixel strength and intensity we can suggest information to the radiologist the spread affects the infected portion to decide on pixel intensity.

$$B = B_{ob}(\emptyset) + B_{ib}(\emptyset) \quad (1)$$

Where

B_{roc} = convex energy concerning the region of contrast

B_{ob} = concave region extraction in outer surface

BE_{ib} = contour region extraction in an inner surface

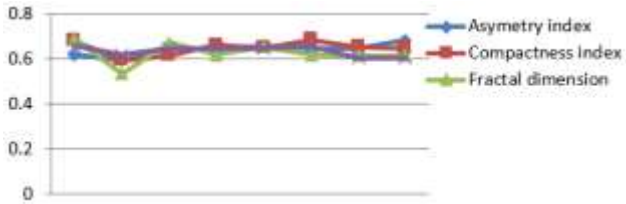

Fig. 7: Parameter extracted for pneumonia in chest X-Ray

Region of interest with convex and concave borders is delineated concerning high clarity in the processed image. The number of pixels also determines the concave region. The concave specifies the region of interest and its spectral properties.

$$B_{ob} = \propto \left[\int_{\Omega} hF(x)\,H_s(\emptyset)\,dx + \int_{\Omega} hFY_{ob}(x)\left(1 - H_s F(\emptyset)\right)dx\right] + \lambda\left[\int_{\Omega} FhZ_{in}(x)\,H_s(\emptyset)\,dx + \int_{\Omega} FhZ_{ob}(x)\left(1 - H_s(\emptyset)\right)dx\right] \quad (2)$$

Where,

$$N(x) = [p(x) - x]^2 \quad (3)$$

$$N_{ob}(x) = [p(x) - x_2]^2 \quad (4)$$

$$Z_{ib} = |E(x) - c_1|^2 + |I(x) - f|^2 \quad (5)$$

$$Z_{ob} = |p(x) - c_2|^2 \quad (6)$$

Table 1 shows the parameter extraction of fever, the parameter asymmetry index, compactness, dimension, and edge are the index specified in the region of concave which enhances high image features for contrast. table 1 shows the convex and concave region extraction and % error present in the input image. The concave region present is extracted with the range of selected dimensions.

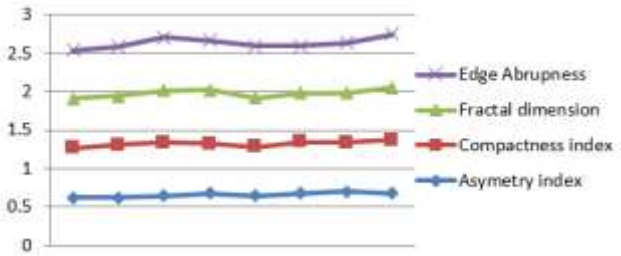

Fig. 8: Parameter extracted for mucus fluid in chest X-Ray

Fig. 3 shows the virus-affected person within 6 days from the extracted parameter of pneumonia. The MCOA clusters the image for the image dimension and range of selection of pixels with inner and outer boundary prediction. The image is processed through certain types of filters where the noise is eliminated to enhance high-contrast clustered images. The clustered image is the noise-free image which reduces pepper and salt noise and improves the accuracy in the solution space. Thus by comparing the fig. from (a) to (h) we find changes in all the images. The changes are enhanced with high image features to obtain the best optimal solution in search space by local optima. When comparing fig. (a) to (e) the portion highlighted in red color indicates some parts of the lungs the infection rate is slightly increased which is highlighted and marked in red color. Furthermore, when comparing fig. (a) to (f) how far the virus affects the lung region and how it spreads randomly. Fig. (g) accurately represents the pixel with the right side of the lungs affected within the region of contrast. By analyzing the pixel strength and intensity we can suggest information to the radiologist the spread affects the infected portion to decide on pixel intensity. Figs. (e) and (f) where the spreading of the virus increases randomly it may cause the entire lung system failed and the prediction of patient health condition is only about 50 % percent and as shown in table 2. Where the infection of the virus in the right side of the lungs is affected and contour edge detection in the concave region is exactly 50%. Statistical table 2 proves for the selected parameter Scaling constants with Heaviside function for pixel information are. Additionally, a boundary edge detector, designated by the symbol h, is embedded with the function of energy.

$$F = \frac{1}{1 + |b_{k_p} * I|^2} \quad (7)$$

Where the gradient operator (r) and the Gaussian kernel (k p) with standard deviation additionally, the convolution operator * lessen the impact of strong noise.

$$P(x) = |\bar{I}(y) - I_k(y)|^2 \quad (8)$$

The image has been blurred with the Gaussian filter where I am the mean pixel value of I and Ik = k* * I. Additionally, the saliency means for "in" and "op" are s1 and s2

$$s_1 = \frac{\int_\Omega p(x).n_\varepsilon(\emptyset)\,dx}{\int_\Omega k_\varepsilon(\emptyset)\,dx} \quad (9)$$

$$s_2 = \frac{\int_\Omega p(x).(1 - k_\varepsilon(\emptyset))\,dx}{\int_\Omega (1 - j_\varepsilon(\emptyset))\,dx} \quad (10)$$

$$c_1 = \omega\ .mean\ (I(x)\ \epsilon\ \Omega_{in})$$
$$c_2 = \omega\ .mean\ (I(x)\ \epsilon\ \Omega_{op})$$
$$f = \omega\ .median\ (I(x)\ \epsilon\ \Omega_{in}) \quad (11)$$

Table 2 shows the parameter extraction of fever, the parameter asymmetry index, compactness, dimension, and edge are the index specified in the region of concave which enhances high image features for contrast. table 1 shows the convex and concave region extraction and % error present in the input image. The concave region present is extracted with the range of selected dimensions.

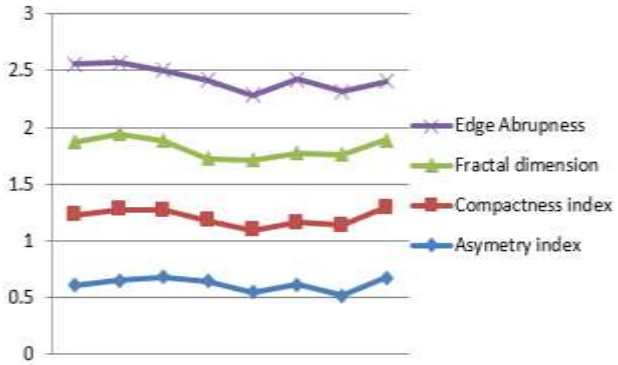

Fig. 9: Parameter extracted for Respiration rate in chest X-Ray

Fig. 4 shows the virus-affected person within 9 days from the extracted parameter of respiration rate. The MCOA clusters the image for the image dimension and range of selection of pixels with inner and outer boundary prediction. The image is processed through certain types of filters where the noise is eliminated to enhance high-contrast clustered images. The clustered image is the

noise-free image which reduces pepper and salt noise and improves the accuracy in the solution space. Thus by comparing the fig. from (a) to (h) we find changes in all the images. The changes are enhanced with high image features to obtain the best optimal solution in search space by local optima. When comparing fig. (a) to (e) the portion highlighted in red color indicates some parts of the lungs the infection rate is slightly increased which is highlighted and marked in red color. Furthermore, when comparing fig. (a) to (f) how far the virus affects the lung region and how it spreads randomly. Fig. (g) accurately represents the pixel with the right side of the lungs affected within the region of contrast. By analyzing the pixel strength and intensity we can suggest information to the radiologist the spread affects the infected portion to decide on pixel intensity. Figs. (e) and (f) where the spreading of the virus increases randomly it may cause the entire lung system failed and the prediction of patient health condition is only about 50 % percent and as shown in table 2. Where the infection of the virus in the right side of the lungs is affected and contour edge detection in the concave region is exactly 50%. Statistical table 2 proves for the selected parameter

$$\omega = \int_{\Omega} f_{\varepsilon}(\emptyset)||p||_2\, dx + \int_{\Omega} (1 - p_{\varepsilon}(\emptyset))\, ||p||_2\, dx \tag{12}$$

The function of energy clustered is inaccurate with irregular shape and edges, and some false contours present in the particular state to detect the error in the input image. Therefore, the function of energy is represented as

$$E_{ib}(\emptyset) = \frac{kl(\emptyset)\, \eta(I)}{\max(|k(I)|)} + \nu P(\emptyset) \tag{13}$$

Where k; ν > 0 constants.

$$l(\emptyset) = \int_{\Omega} h\delta_{\varepsilon}(\emptyset)|\nabla_{\emptyset}|\, dx \tag{14}$$

$$P(\emptyset) = \int_{\Omega} \frac{1}{2}(1 - |\nabla_{\emptyset}|)^2\, dx \tag{15}$$

Table 3. shows the parameter extraction of mucus fluid, the parameter are asymmetry index, compactness, dimension, and edge are the index specified in the region of concave which enhances high image features for contrast. table 1 shows the convex and concave region extraction and % error present in the input image. The concave region present is extracted with the range of selected dimensions.

Fig. 5 shows the virus-affected person within 9 days from the extracted parameter of respiration rate. The MCOA clusters the image for the image dimension and range of selection of pixels with inner and outer boundary prediction. The image is processed through certain types of filters where the noise is eliminated to enhance high-contrast clustered images. The clustered image is the noise-free image which reduces pepper and salt noise and improves the accuracy in the solution space. Thus by comparing the fig. from (a) to (h) we find changes in all the images. The changes are enhanced with high image features to obtain the best optimal solution in search space by local optima. When comparing fig. (a) to (e) the portion highlighted in red color indicates some parts of the lungs the infected rate is slightly increased which is highlighted and marked in red color. Furthermore, when comparing fig. (a) to (f) how far the virus affects the lung region and how it spreads randomly. Fig. (g) accurately represents the pixel with the right side of the lungs affected within the region of contrast. By analyzing the pixel strength and intensity we can suggest information to the radiologist the spread affects the infected portion to decide on pixel intensity. Figs. (e) and (f) where the spreading of the virus increases randomly it may cause the entire lung system failed and the prediction of the patient's health condition is only about 50 % percent and as shown in Table 2. Where the infection of the virus in the right side of the lungs is affected and contour edge detection in the concave region is exactly 50%. Statistical table 2 proves for the selected parameter

$$\eta(I) = sgn(2c_1 + 2f - 4c_2).sgn\,(\gamma).\gamma^2 \tag{16}$$

Where

$$\gamma = I(x) - \frac{c_1^2 + f^2 - 2c_2^2}{2c_1 + 2f - 4c_2} \tag{17}$$

The symptoms of COVID-19 in an X-ray image, the infection occurs within 9 days as shown in fig. 4. From input, the X-ray image is clustered and forecasts COVID-19 spread ability. To make an accurate forecast of virus spread the clustering is defined with a certain parameter for high accuracy. Comparatively, the frequency portion is muted, and COVID-19 extraction is calibrated to accurately detect the virus. X-ray picture segmentation of the chest that includes the crucial details on the virus spread throughout the lungs. Since the virus's affection is so dangerous, the segmentation algorithm's COVID-19 analysis should catch it early.

Table 4 shows the parameter extraction of respiration rate, the parameter is asymmetry index, compactness, dimension, and edge are the index specified in the region of concave which enhances high image features for contrast. table 1 shows the convex and concave region extraction and % error present in the input image. The concave region present is extracted with the range of selected dimensions.

RESULT

The relationship between COVID-19 symptoms is depicted in fig. (6) through (9), both with and without contour detection in the region of concave. The fig. (6)

curve that distinguishes between pneumonia, mucus fluid, fever, respiration rate and COVID-19 is plotted to show the accuracy of delineation. In fig. (6) the parameter suggested and shows compactness index and dimension are merging i.e. means the concave region detected in the chest x-ray image proves its accuracy to be 50% in the state of the art in the solution space. In fig. (7) the parameter suggested and shows compactness index and dimension are merging i.e. means the concave region detected in the chest x-ray image proves its accuracy to be 70% in the state of the art in the solution space. In fig. (6) the parameter suggested and shows compactness index and dimension are not merging i.e. means the concave region detected in the chest x-ray image proves its accuracy to be 80% in the state of the art in the solution space.

DISCUSSION

COVID-19 pandemic identifies the epidemic cases increases all over the world. In order to control the spreading of epidemics certain techniques needs to be followed and also to maintain social distance. There is certain response to control the disease and exposed to healthy effects in terms of societal solution to tackle epidemic vulnerability. Nowadays vaccines are available to increase the immunity power to control the epidemics but this is not 100% solution to control the epidemics. The All India Council for Medical Education needs to take certain steps about COVID epidemic in earlier stage. The overall solution to stop the epidemic in earlier stage and diagnose through modified CAT optimization algorithm both in seeking and tracing mode. The tracing mode highlights the social behavior as well as clusters the process through the non-convex border in chest X-Ray imaging and finally given the solution to stop the epidemics. Furthermore, the Chest X-Ray Imaging processed through optimization algorithm delineate the virus spread from the day 1 to end day.

CONCLUSION

The mortality rate is accurately predicted by segmenting a chest X-ray image that has been improved for feature extraction and assessment. The virus is rapidly spreading, making it crucial to correctly identify COVID-19's symptoms. The suggested segmentation approach accurately and uncritically validates the COVID-19 symptoms using ground truth verification. Without adequate information regarding COVID-19, it can be challenging to diagnose the disease's symptoms, but the segmentation algorithm's new approach employing chest X-ray imaging turns out to be an effective one. To diagnose a patient with COVID-19, the chest X-ray imaging resolution range is relatively limited. The patient can have a virus-free life because of the early diagnosis prediction of COVID-19.

REFERENCES

Djuric O, Ottone M, Vicentini M, Venturelli F, Pezzarossi A, Manicardi V, Greci M, Giorgi P, Group EC, Formoso G, Bedeschi E, Perilli C, Venturi I, Bisaccia E, Larosa E, Cassinadri M, Cilloni S and Campari C (2022). Diabetes Research and Clinical Practice Diabetes and COVID-19 testing, positivity, and mortality : A population-wide study in Northern Italy. 191.

Erdem K and Duman A (2022). Pulmonary Artery pressures and right ventricular dimensions of post-covid-19 patients without previous significant cardiovascular pathology. *Heart & Lung*, **57**(313): 75-79.

Friedman-Klebanoff DAJ, Tjaden AH, Santacatterina M, Munawar I, Sanders JW, Herrington DM, Wierzba TF and Berry AA (2022). Vaccine-induced seroconversion in participants in the North Carolina COVID-19 community research partnership. *Vaccine*, **40**(42): 6133-6140.

Lo E, Nuzzo D, Al W, Al-rasadi K, Al-alawi K, Banach M, Banerjee Y, Ceriello A, Cesur M, Cosentino F, Firenze A, Galia M, Goh S, Janez A, Kalra S, Kapoor N, Kempler P, Lessan N, Lotufo P and Capisco SC (2022). BBA - Molecular basis of disease molecular and pro-inflammatory aspects of COVID-19: The impact on cardiometabolic health.

Materassi M (2019). Some fractal thoughts about the COVID-19 infection outbreak., **4**(100032): 0-5.

McEniery CM, Fisk M, Miles K, Kaloyirou F, Hubsch A., Smith J, Wilkinson IB and Cheriyan J (2020). Erratum: ChemoPROphyLaxIs with hydroxychloroquine for covId-19 infeCtious disease (PROLIFIC) to prevent covid-19 infection in frontline healthcare workers: A structured summary of a study protocol for a randomized controlled trial., **21**(1): 13063.

Mohammed T, Brewer JVV, Pyatt M, Whitbourne SB, Gaziano JM, Edson C and Holodniy M (2022). Evaluation of independent self-collected blood specimens for COVID-19 antibody detection among the US veteran population. *Diagn. Microbiol. Infect. Dis.*, **104**(2): 115770.

Sokas C, Kelly M, Sheu C, Song J, Welch HG, Bergmark, R, Minami C and Trinh QD (2021). ASO Visual Abstract: Cancer in the shadow of COVID: Early-stage breast and prostate cancer patient perspectives on surgical delays due to COVID-19. **28**(s3): 545.

Suy A, Garcia-Ruiz I, Carbonell M, Garcia-Manau P, Rodo C, Maiz N, Sulleiro E, Anton A, Esperalba J, Fernández-Hidalgo N, Frick MA, Camba F, Pumarola, T, Carreras E, García-Ruiz I, Maiz N, Mendoza M, Illan L, Fernandez-Blanco L and Mateos S (2021). Gestation and COVID-19: Clinical and microbiological observational study (Gesta-COVID19). *BMC Pregnancy and Childbirth*, **21**(1): 4-9.

Weller M and Preusser M (2020). How we treat patients

with a brain tumor during the COVID-19 pandemic. *ESMO Open*, **4**(2): 19-21.

Wilke LG, Nguyen TT, Yang Q, Hanlon BM, Wagner KA, Strickland P, Brown E, Dietz JR and Boughey JC (2021). ASO visual abstract: Analysis of the impact of the COVID-19 pandemic on the multidisciplinary management of breast cancer-review from the american society of breast surgeons COVID-19 and mastery registries. *Ann. Surg. Oncol.*, **28**(s3): 630.

Arias-Londono JD, Gomez-Garcia JA, Moro-Velazquez L and Godino-Llorente JI (2020). Artificial intelligence applied to chest X-Ray images for the automatic detection of COVID-19. A thoughtful evaluation approach. *IEEE Access*, **8**: 226811-226827.

Dong D, Tang Z, Wang S, Hui H, Gong L, Lu Y and Li H (2021). The Role of imaging in the detection and Management of COVID-19: A Review. *IEEE Rev. Biomed. Eng.*, **14**: 16-29.

Gharizadeh B, Yue J, Yu M, Liu Y, Zhou M, Lu D and Zhang J (2021). Navigating the pandemic response life cycle: molecular diagnostics and immunoassays in the context of COVID-19 management. *IEEE Rev. Biomed. Eng.*, **14**(1): 30-47.

Jiang Y, Chen H, Loew M and Ko H (2021). COVID-19 CT image synthesis with a conditional generative adversarial network. *IEEE J. Biomed. Health Inform.*, **25**(2): 441-452.

Joshi A, Khan MS, Soomro S, Niaz A, Han BS and Choi KN (2020). SRIS: Saliency-based region detection and image segmentation of COVID-19 infected cases. *IEEE Access*, **8**(1): 190487-190503.

Karadayi Y, Aydin MN and Ogrenci AS (2020). Unsupervised anomaly detection in multivariate Spatio-temporal data using deep learning: Early detection of a covid-19 outbreak in Italy. *IEEE Access*, **8**: 164155-164177.

Liu Q, Leung CK and Hu P (2020). A two-dimensional sparse matrix profile densenet for COVID-19 diagnosis using chest ct images. *IEEE Access*, **8**(1): 213718-213728.

Marmarelis VZ (2020). Predictive modeling of covid-19 data in the us: adaptive phase-space approach. *IEEE Open J. Eng. Med. Biol*., **1**: 207-213.

Peng Y, Tang Y, Lee S, Zhu Y, Summers RM and Lu Z (2021). COVID-19-CT-CXR: A freely accessible and weakly labeled chest X-Ray and CT image collection on COVID-19 from biomedical literature. *IEEE Transactions on Big Data*, **7**(1): 3-12.

Rajaraman S, Siegelman J, Alderson PO, Folio LS, Folio LR and Antani SK (2020). Iteratively pruned deep learning ensembles for COVID-19 detection in chest X-Rays. *IEEE Access*, **8**(1): 115041-115050.

Sakib S, Tazrin T, Fouda MM, Fadlullah ZM and Guizani M (2020). DL-CRC: Deep learning-based chest radiograph classification for COVID-19 detection: A novel approach. *IEEE Access*, **8**(1): 171575-171589.

Shi J, Yuan X, Elhoseny M and Yuan X (2020). Weakly supervised deep learning for object detection from images, **8**: 231-242.

Su Z, Pahlavan K and Agu E (2021). Performance evaluation of COVID-19 proximity detection using bluetooth le signal. *IEEE Access*, pp.38891-38906.

Tabik S, Gomez-Rios A, Martin-Rodriguez JL, Sevillano-Garcia I, Rey-Area M, Charte D and Herrera F (2020). COVIDGR dataset and covid-zdnet methodology for predicting covid-19 based on chest X-Ray images. *IEEE J. Biomed. Health Inform.*, **24**(12): 3595-3605.

Waheed A, Goyal M, Gupta D, Khanna A, Al-Tudjman F and Pinheiro PR (2020). CovidGAN: Data augmentation using auxiliary classifier gan for improved COVID-19 detection. *IEEE Access*, **8**(1): 91916-91923.